Design, Synthesis, and Biological Evaluation of Antiviral Agents Targeting Flavivirus Envelope Proteins

Ze Li,[†] Mansoora Khaliq,[‡] Zhigang Zhou,[†] Carol Beth Post,[†] Richard J. Kuhn,[‡] and Mark Cushman*[,†]

Department of Medicinal Chemistry and Molecular Pharmacology, School of Pharmacy and Pharmaceutical Sciences and the Purdue Cancer Center, Purdue University, West Lafayette, Indiana 47907, Department of Biological Sciences, Purdue University, West Lafayette, Indiana 47907

Received April 10, 2008

Flavivirus envelope proteins (E proteins) have been shown to play a pivotal role in virus assembly, morphogenesis, and infection of host cells. Inhibition of flavivirus infection of a host cell by means of a small molecule envelope protein antagonist is an attractive strategy for the development of antiviral agents. Virtual screening of the NCI chemical database using the dengue virus envelope protein structure revealed several hypothetical hit compounds. Bioassay results identified a class of thiazole compounds with antiviral potency in cell-based assays. Modification of these lead compounds led to a series of analogues with improved antiviral activity and decreased cytotoxicity. The most active compounds **11** and **36** were effective in the low micromolar concentration range in a cellular assay system.

Introduction

Many flaviviruses are arthropod-borne, human pathogens that can cause encephalitis, hemorrhagic fever, shock syndrome, and jaundice. Examples of pathogenic flaviviruses include dengue virus, yellow fever virus, West Nile virus, tick-borne encephalitis virus, and Japanese encephalitis virus. A number of antiflaviviral agents with a wide variety of putative targets have been reported, including those that act on viral membranes,[1] translation,[2] c-Src protein kinase,[3] RNA[a] polymerase,[4] α-glucosidase,[5,6] mRNA,[7] cellular IMP dehydrogenase,[8] 2′-*O*-methyltransferase,[9] and RNA-dependent RNA polymerase.[10] In addition, peptide antiviral agents targeting West Nile virus envelope protein (E protein) have been reported to be active against both dengue virus and West Nile virus.[11] However, at the present time, there are no clinically useful antiflaviviral agents.

The flaviviruses infect host cells through receptor-mediated endocytosis to form a virus-containing endosome, followed by fusion of the viral envelope with the host cell membrane.[12] The fusion process is orchestrated by the viral E proteins, which are made up of three domains: domain I (DI), the middle domain, is attached at one end to domain II (DII), the fusion domain, and at the other end contacts domain III (DIII), the receptor binding domain (Figure 1).[13] Domain II contains the fusion peptide loop near its tip, which is inserted into the host cell membrane after the E protein undergoes a series of conformational changes.

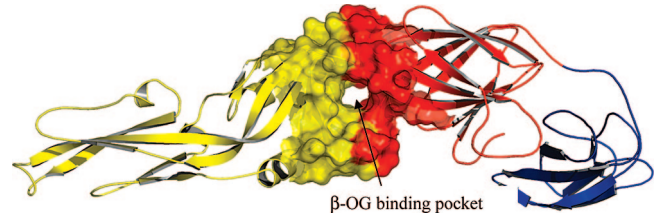

Figure 1. Structure of dengue 2 E protein. Domain I: red; domain II: yellow; domain III: blue. The β-OG binding pocket is located between domains I and II.

Cryo-electron microscopy and X-ray crystallography studies of various flavivirus E protein fragments have revealed that domains I and II are connected by a mobile hinge that allows rotation of DII relative to DI−DIII during the processes of viral maturation and fusion of the viral envelope with the host cell membrane.[14–17] Mutations that affect the pH threshold for either fusion or virulence are clustered in this hinge region.[18–23] Furthermore, crystallization of a dengue virus type 2 E protein fragment in the presence of the detergent *n*-octyl-β-D-glucoside (β-OG) has led to structures with and without occupation of the hinge pocket by β-OG.[14] Occupation of the pocket by β-OG requires an altered conformation of the kl loop toward an "open" position, and the angle that DII makes with DI−DIII also differs between two crystal structures with and without β-OG.[14] The β-OG pocket may therefore represent an ideal target for structure-based design of potential antiviral agents because ligands that bind there could alter the conformational equilibrium associated with the hinge angle and inhibit virus maturation.[14,15] Moreover, the effect on hinge equilibrium could interfere with the fusion of the viral envelope with the host cell membrane.

Computational screening of an NCI library using the β-OG binding pocket recently identified a small set of compounds that were predicted to bind in the pocket. An array of 23 compounds were selected for antiviral testing vs yellow fever virus replication. Of these, nine compounds inhibited viral growth and several of them had EC_{50} values in the micromolar range and were potent enough to warrant further consideration. These

* To whom correspondence should be addressed. Phone: +1 765 494 1465. Fax: +1 765 494 6790. E-mail: cushman@pharmacy.purdue.edu.

[†] Department of Medicinal Chemistry and Molecular Pharmacology, School of Pharmacy and Pharmaceutical Sciences and the Purdue Cancer Center, Purdue University.

[‡] Department of Biological Sciences, Purdue University.

[a] Abbreviations: RNA, ribonucleic acid; mRNA, messenger ribonucleic acid; IMP, inosine monophosphate; NCI, National Cancer Institute; SAR, structure−activity relationship; DMSO-d_6, hexadeuterodimethyl sulfoxide; NMR, nuclear magnetic resonance; TMS, tetramethylsilane; HRMS, high resolution mass spectrum; ES+, positive ion electrospray; EDCI, 1-ethyl-3-(3-dimethylaminopropyl)carbodiimide; DMF, dimethylformamide; NBS, *N*-bromosuccinimide; YFV, yellow fever virus; IRES, internal ribosome entry site; Luc, luciferase; 3′ NTR, 3′ nontranslated region; PCR, polymerase chain reaction; EMCV, encephalomyocarditis virus; MEM, minimum essential medium; FBS, fetal bovine serum; BHK, baby hamster kidney, PBS, phosphate-buffered saline; NIH, National Institutes of Health; NIAID, National Institute of Allergy and Infectious Diseases; RCE, Regional Centers of Excellence.

10.1021/jm800412d CCC: $40.75
Published on Web 07/09/2008

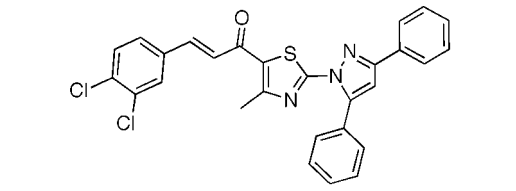

M02
EC_{50} = 51 ± 7.2 uM
CC_{50} = 70 ± 12 uM

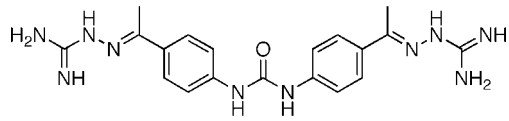

P02
EC_{50} = 13 ± 3 uM
CC_{50} = 398 ± 0.1 uM

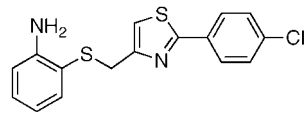

D03
EC_{50} = 31 ± 0.3 uM
CC_{50} = 61 ± 3 uM

Figure 2. Chemical structures of the "hits" identified through in silico screening and biological evaluation. The antiviral activities were determined using yellow fever virus.

three hit compounds, **M02**, **P02**, and **D03** (Figure 2), provided a starting point for lead optimization in the present study.

Design

The binding models derived from docking results indicate that compounds **M02** and **P02** might bind to the E protein β-OG binding site in a similar way. An overlay of their docked models suggested that these molecules occupy a pocket that is located in the hinge region between domains I and II (Figure 1). Computational analysis revealed that the middle part of the pocket is the most hydrophobic and the entrance part is the most hydrophilic (Figure 3). The bottom region of the pocket contains some hydrophilic amino acid residues that could interact with ligands through electrostatically favorable interactions as in the case of **P02**. One end of the ligand can reach into the pocket, and electrostatically favorable interactions could be formed between the aminoguanidine groups with Thr280 in domain I and Asp203, Gln200, Gln271, and Ser274 in domain II (Figure 4B). Topologically, the entrance of the pocket shows a rather wide space in which the ends of the hit compounds assume various positions, whereas the middle part of the pocket has the most limited space.

An analysis of the protein−ligand interaction suggests that tight-binding inhibitors might be obtained by grafting half of the structure of **P02** onto half of the structure of **M02**. Driven by the hypothesis that the aminoguanidine group in **P02** can potentially form electrostatically favorable interactions with the residues in the receptor pocket, one-half of the structure of **P02** was incorporated by connecting it to **M02**'s thiazole ring, which is a common structural feature that many of the hits contain. This contributed to the design of the first two target compounds **1** and **2** (Figure 5). The double bond in the α,β-unsaturated ketone present in inhibitor **M02** is electrophilic and could react nondiscriminately with biological nucleophiles, thus resulting in toxicity. Accordingly, in the design of the first two potential inhibitors, this moiety was replaced with a bioisosteric amide linkage. The Figure 5 depicts compounds **1**, **2**, and their analogues **3**−**8**, which have been synthesized and bioassayed.

According to the docked models of the hit **M02**, one of the two phenyl rings attached to the 3,5-diphenyl-1*H*-pyrazole was calculated to point to an independent hydrophobic region. This phenyl ring has been thought to be redundant and was deleted in our first generation drug design because no comparable partial structures in the other hits can overlay with this group in the docked models. However, considering the fact that this phenyl ring may nevertheless play an important role in the hit's antiviral activity, a class of compounds based on the structure of the hit **M02** has been designed, synthesized, and bioassayed (Figure 6). The only modification in structure **11** is that the α,β-unsaturated ketone in **M02** has been replaced by a bioisosteric amide, which was based on the same considerations with regard to toxicity as described above. To clarify the role of the 3,5-diphenyl-1*H*-pyrazole moiety of **M02** in its antiviral activity, 3,5-diphenyl-1*H*-pyrazole (**17**) itself was tested for antiviral activity.

By comparing the docked models of **P02** and **M02**, a class of branched compounds (**18**, **19**, and **20**, Figure 7) was designed, synthesized, and bioassayed. These compounds can be considered as analogues in which a derivative of the substituted thiazole moiety of **M02** has been attached to a fragmented analogue of **P02**.

Another class of compounds was designed to mimick the hit **D03**, which provides a convenient template for diversification. An array of analogues of **D03** shown in Figure 8 has therefore been synthesized and bioassayed. It was expected that these structurally related compounds could provide useful SAR information.

A final set of compounds was derived from fragments of **M02** and **D03** (Figure 9). The phenylthiazole moiety of **D03** was attached to an analogue of the 3,4-dichlorostyryl moiety of **M02**, resulting in **34**. Introduction of bromine into the methyl group of **32** led to the dibromosubstituted compound **36**. This compound, showing unexpected stability, presented an interesting chemical probe to test the influence of electronic and steric effects on antiviral activity.

Synthesis

The synthetic route to compounds **1**−**8** is outlined in Scheme 1. Radical bromination of methyl 3-oxobutanoate (**37**) was used to construct methyl 2-bromo-3-oxobutanoate (**38**),[24] which reacted with thiourea at room temperature to give rise to the thiazole intermediate, 2-amino-4-methylthiazole-5-carboxylic acid methyl ester (**39**).[25] Reaction of this intermediate with 1-(4-isocyanatophenyl)ethanone in pyridine afforded compound **3**. Hydrolysis of **3** with sodium hydroxide to the corresponding acid **4** and then amidation with 2,4-dichloro- or 3,4-dichlorobenzylamine mediated by 1-ethyl-3-(3′-dimethylaminopropyl)carbodiimide (EDCI) readily provided the desired compounds **7** and **8**. Target hydrazones **1** and **2** were synthesized by reacting **7** with semicarbazide hydrochloride or aminoguanidine hydrochloride, respectively.[26] Compounds **5** and **6** were prepared from **3** similarly.

Compounds **9**−**16** were synthesized through the route shown in Scheme 2, in which a copper-catalyzed N-arylation reaction of the pyrazole **17** is the key step.[27] The reaction is highly sensitive to air. In our experiments, the reaction was conducted in a sealed pressure vessel filled with argon gas. Conversions of **10** to **11**−**16** were performed smoothly.

The branched potential inhibitors **18**–**20** were made as outlined in Scheme 3. Bisalkylation of 2-amino-4-methylthiaz-

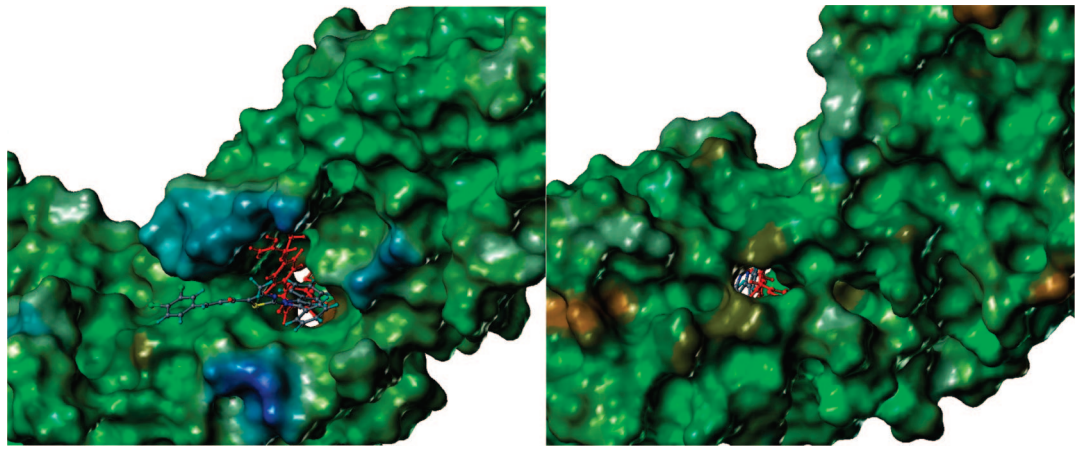

Figure 3. Lipophilic potential analysis of the E protein β-OG binding site showing the entrance region is relatively more hydrophilic and the middle region is the most lipophilic region. The lipophilic potential ranges from −0.241 (blue, hydrophilic) to 0.147 (brown, hydrophobic). The left picture views the pocket from entrance side, and the right picture views the pocket from the bottom side. The red stick model is **P02** and the stick model colored by atom type is **M02**.

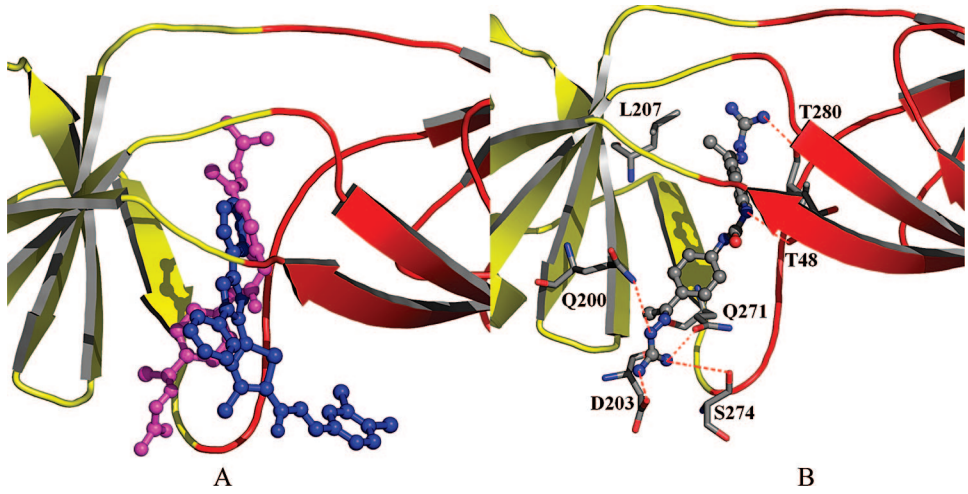

Figure 4. (A) Two active compounds docked in the β-OG pocket of dengue E protein. The structure colored magenta is **P02**, and the structure colored blue is **M02**. (B) Potential electrostatically favorable interactions formed between residues Asp203, Gln200, Gln271, Ser274, Thr48, and Thr280 with **P02**. Part of the protein is shown in cartoon representation with red color for domain I and yellow color for domain II.

ole-5-carboxylic acid methyl ester (**39**) with 1-(4-(bromomethyl)-phenyl)ethanone (**41**) was performed with sodium hydride as the base to afford **18**. In the presence of ethyl acetate, the major product of the reaction was **20**. Compound **18** was further converted to **19** through the acid **42** via a hydrolysis−amidation sequence similar to the synthetic route to compounds **10** and **11**.

Analogues of **D03** were prepared following the routes depicted in Scheme 4. Heterocyclic ring closure of 4-chlorothiobenzamide (**43**) with 1-chloroacetone (**44**) afforded compound **21**. Reaction of 1,3-dichloroacetone (**45**) with aromatic thioamides, followed by nucleophilic substitution of the chloride intermediates with thiophenols, readily provided **23**−**30** in good yield.[28,29]

Potential inhibitors **31**−**36** were obtained by the route detailed in Scheme 5. Heterocyclic ring closure of arylthioamides with 2-chloro-3-oxo-butyric acid methyl ester (**46**)[30,31] furnished compounds **31**−**33**. Hydrolysis of **32** to the corresponding acid and then amidation or esterification afforded compounds **34** and **35**. Bromination of **32** with NBS provided the dibromosubstituted product **36**.

Biological Results and Discussion

All of the compounds were evaluated in a yellow fever virus inhibition assay (see Experimental Section). The compounds that showed over 50% inhibitory activity on viral replication at a concentration of 50 μM were considered to be active and were tested to determine their EC_{50} and CC_{50} values. The biological data are summarized in Table 1.

Bioassay results showed that compounds **2**, **3**, and **8** exhibited better antiviral activity against yellow fever virus replication in a cellular bioassay system than the parent compounds **M02**, but they were not more potent than **P02**. The results suggest that a core structure consisting of a thiazole ring and an aromatic ring linked by a urea moiety could be a promising structural template for potential antiviral agents. The activity of **3** appears to be structurally specific. For instance, compound **3** lost its activity upon being hydrolyzed to the corresponding acid **4**. In addition, compounds **1** and **7** are inactive vs the active compounds **2** and **8**, even though the structures are very similar. Although the bioassay results revealed several active compounds in this class, their potencies are still moderate.

Although most of the compounds in the **9**−**16** array did not show over 50% inhibition of virus production at a concentration of 50 μM, the target molecule **11** showed enhanced antiviral activity and decreased cytotoxicity compared with the parent compound **M02**. The antiviral activity of **11** (EC_{50} 5 ± 1.7 μM) is 10 times that of parent compound and cytotoxicity is 2.7 times less, resulting in a therapeutic index of 37. These data validate

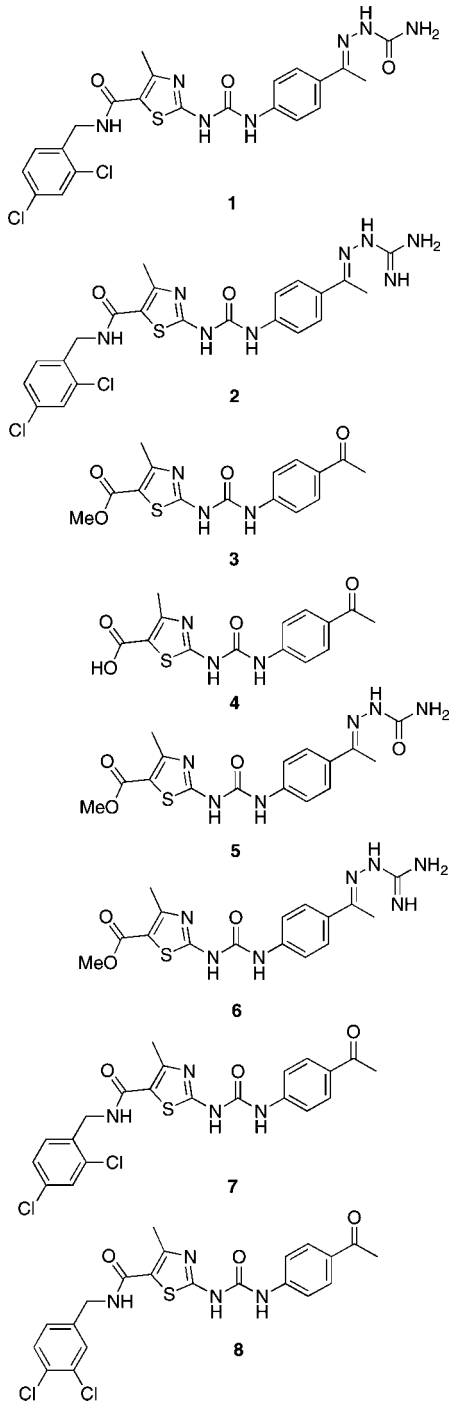

Figure 5. The first generation of designed molecules **1** and **2** and analogues.

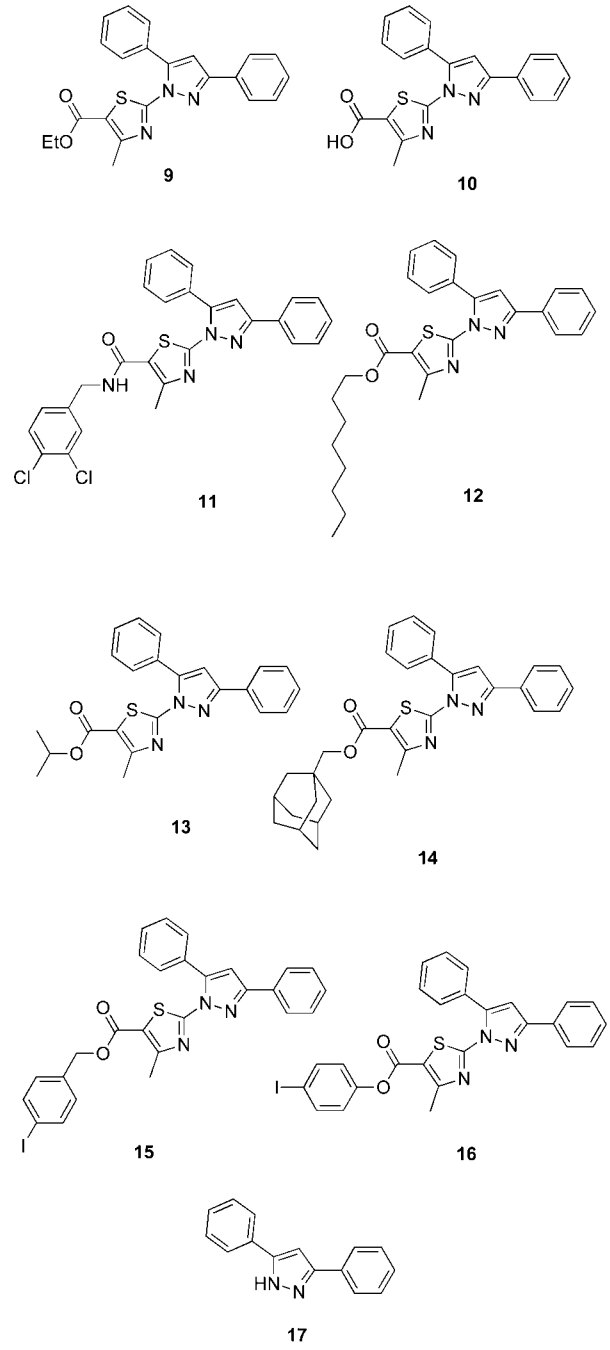

Figure 6. Analogues of **M02**.

the hypothesis that replacing the Michael acceptor in **M02** with a bioisosteric amide would reduce the undesired cytotoxicity. The weak antiviral activities of the other analogues may indicate that an aromatic substituent attached to the thiazole ring through a stable linker such as an amide is necessary for optimal antiviral activity. The hydrolytic instability of the ester linker could explain why the ester analogues, such as compounds **12**−**16**, did not display antiviral activity. Obviously, the amide **11** should be more stable than the esters to enzymatic hydrolysis. Testing the contribution of the 3,5-diphenyl-1*H*-pyrazole moiety to antiviral activity of **M02** revealed that the 3,5-diphenyl-1*H*-pyrazole (**17**) fragment is at least as active as the parent **M02** (EC_{50} 44 vs 51 μM).

Bioassay results showed that the branched compound **18** is active against yellow fever virus, with an EC_{50} value of 25 μM. The results suggest that replacement of the diphenylpyrazole moiety of structure **M02** with tertiary amines could be a possible strategy to develop more potent flavivirius inhibitors.

Compounds **23**−**27** mimicking **D03** exhibited antiviral activity at 30−50 μM range, which is comparable to the activity of **D03** itself (EC_{50} 31 μM). It seems that the overall physical−chemical properties of the compounds are the determining factor for their biological activity. Slight modifications in structure do not cause a significant change in antiviral activity. A preliminary SAR analysis suggested that an electron-rich aromatic ring attached to a thiazole ring that is linked to a 2- or 4-substituted aniline group may represent a template for antiviral agents. The presence of a pyridine

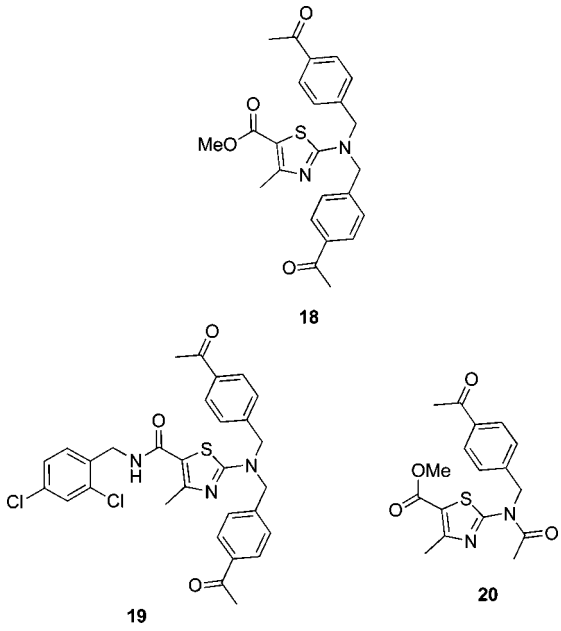

Figure 7. The branched potential flavivirus inhibitors.

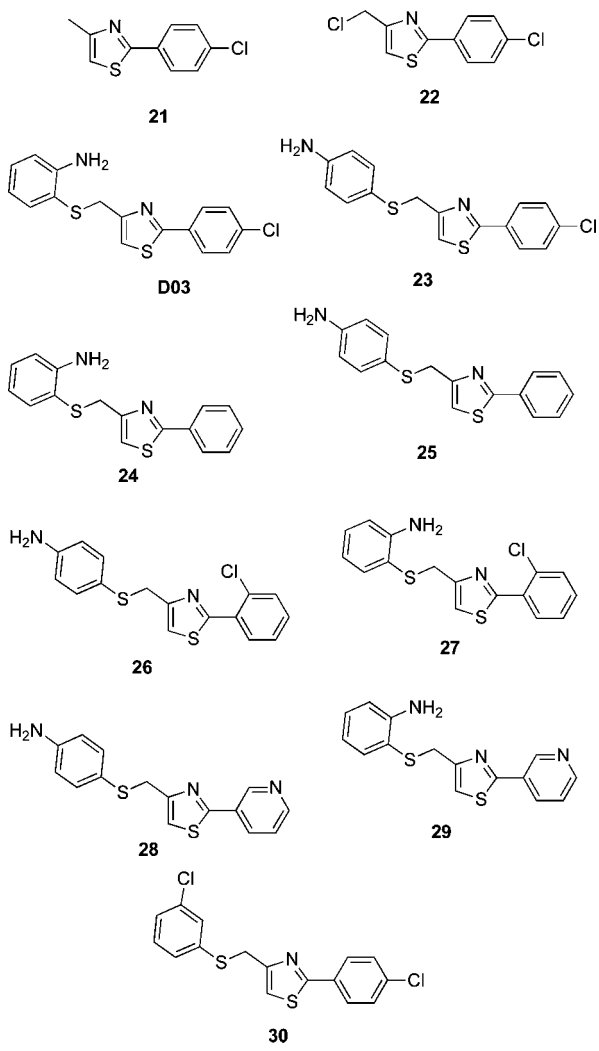

Figure 8. The analogues of **D03**.

ring, such as in compounds **28** and **29**, or the absence of the aniline group, such as in compound **30**, causes these analogues to lose antiviral activity.

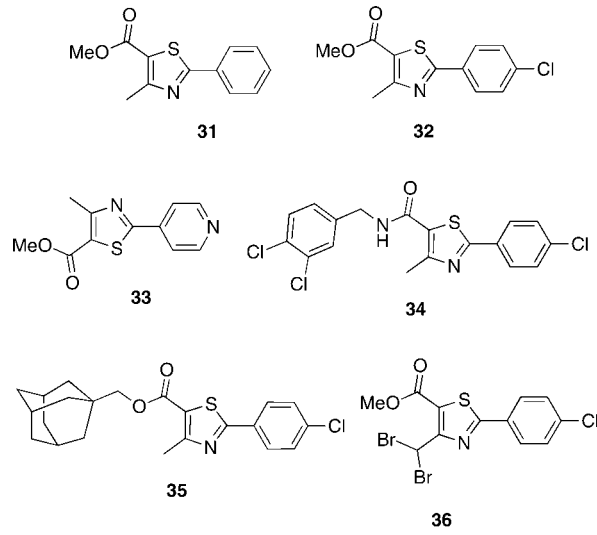

Figure 9. Analogues of **M02** and **D03**.

Scheme 1[a]

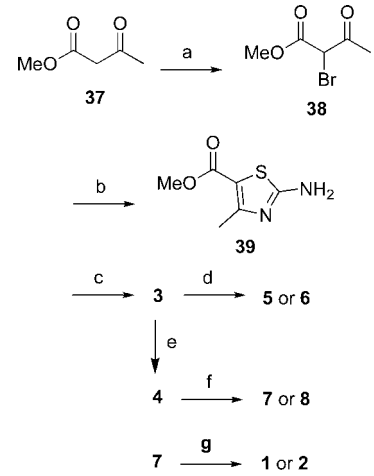

[a] Reagents and conditions: (a) NBS, benzene, AIBN, RT for 2 h, 100%; (b) thiourea, ethanol, RT for 3 h, 81%; (c) 1-(4-isocyanatophenyl)ethanone, pyridine, RT for 12 h, 83%; (d) semicarbazide hydrochloride for **5** or aminoguanidine hydrochloride for **6**, ethanol,triethylamine for **5**, AcOH, heated to reflux for 6 h, 70% for **5**, and 65% for **6**; (e) NaOH, EtOH,MeOH, heated to reflux for 3 h, 73%; (f) 2,4-dichlorobenzylamine for **7** or 3,4-dichlorobenzylamine for **8**, EDCI, pyridine, RT for 12 h, 60−70%; (g) semicarbazide hydrochloride for **1** or aminoguanidine hydrochloride for **2**, ethanol, triethylamine for **1**, AcOH, heated to reflux for 6 h, 73% for **1**, and 67% for **2**.

The most active compound was **36**, which showed 99% inhibition of yellow fever virus and dengue virus replication at the initial 50 μM concentration tested. The EC_{50} value of the compound is 0.9 μM vs yellow fever virus replication. Encouragingly, although this compound contains a dibromomethyl substituent on the thiazole ring that was considered to be likely to cause toxicity by alkylating biological nucleophiles, it was in fact not very cytotoxic (CC_{50} 153 μM), resulting in a good therapeutic index of 170. Obviously, this compound provides an intriguing lead that deserves further study. Comparing the structure of **36** with the others in this class, it seems that the dibromomethyl substituent is important for antiviral activity. Compound **32**, the synthetic precursor of **36**, is inactive against yellow fever virus and it does not contain the dibromomethyl substituent.

The most promising compounds **11** and **36** were docked in the dengue virus E protein β-OG binding pocket in order to

Scheme 2[a]

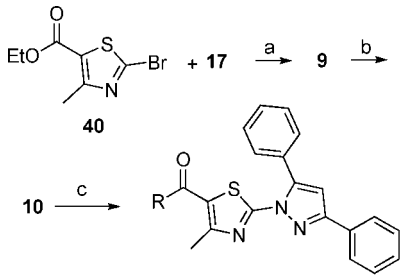

11, R = 3,4-dichlorobenzylamino
12, R = 1-octyloxy
13, R = isopropoxy
14, R = 1-adamantylethyloxy
15, R = 4-iodobenzyloxy
16, R = 4-iodophenoxy

[a] Reagents and conditions: (a) Cu_2O, 2-hydroxybenzaldehyde oxime, $CsCO_3$, CH_3CN, argon, 80−90 °C for 8 h, 65%; (b) LiOH, methanol, ethanol, H_2O, heated to reflux for 3 h, 80%; (c) benzylamines or alkyl alcohols, EDCI, pyridine, RT for 12 h, 60−70%.

Scheme 3[a]

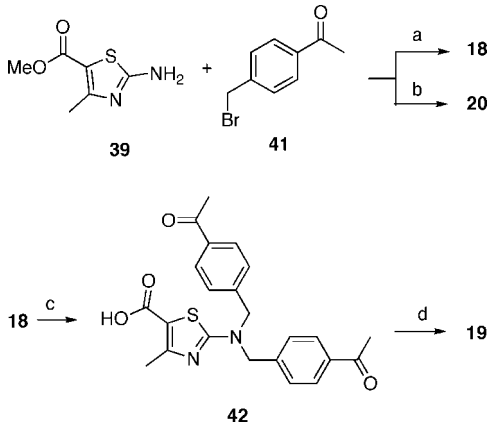

[a] Reagents and conditions: (a) NaH, DMF, 0 °C−RT for 4 h, 74% (b) NaH, DMF, ethyl acetate, 0 °C−RT for 4 h, 70%; (c) NaOH, methanol, ethanol, heated to reflux for 1 h, 70%; (d) 2,4-dichlorobenzylamine, EDCI, pyridine, RT for 12 h, 72%.

gain insight into their probable binding modes (Figure 10). These two compounds may bind in the β-OG binding pocket in an area surrounded by amino acid residues including Thr280, Val130, Leu198, Gln200, Ala205, Ile270, Ser274, Gln271, Leu277, Lys47, Thr48, Glu49, Leu135, Ala50, and Thr137. The entire binding site forms a channel. Compound **11** places its 3,5-diphenyl-1*H*-pyrazole group in the middle region, leaving its amide tail positioned in the entrance region. It is still unclear what role the second phenyl ring of the 3,5-diphenyl-1*H*-pyrazole in compound **11** plays in its antiviral activity. The docked model suggests that this phenyl ring, with its bulky size, could block the compound from docking deeply into the channel. The smaller compound **36** has been suggested by docking simulation to bind deeply into the channel. The binding could be tighter than other compounds binding to the entrance and middle regions, thus resulting in stronger potency. The dibromomethyl substituent of compound **36**, as the biological data indicate, is likely to be a key structural element for the antiviral activity. One bromine atom may hinder nucleophilic displacement of the other bromine atom by biological nucleophiles, thus lowering the cytotoxicity. On the other hand, the docked model suggests that one of the bromine atoms may fit a small region between the entrance region and the middle region. The

Scheme 4[a]

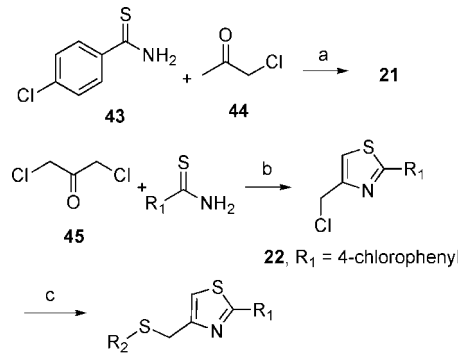

D03, R_1 = 4-chlorophenyl, R_2 = 2-aminophenyl
23, R_1 = 4-chlorophenyl, R_2 = 4-aminophenyl
24, R_1 = phenyl, R_2 = 2-aminophenyl
25, R_1 = phenyl, R_2 = 4-aminophenyl
26, R_1 = 2-chlorophenyl, R_2 = 4-aminophenyl
27, R_1 = 2-chlorophenyl, R_2 = 2-aminophenyl
28, R_1 = 3-pyridyl, R_2 = 4-aminophenyl
29, R_1 = 3-pyridyl, R_2 = 2-aminophenyl
30, R_1 = 4-chlorophenyl, R_2 = 3-chlorophenyl

[a] Reagents and conditions: (a) ethanol, heated to reflux for 2 h, 80%; (b) ethanol, heated to reflux for 2 h, 65%; (c) R_2SH, $CsCO_3$, DMF, 80 °C for 2 h, 70−80%.

Scheme 5[a]

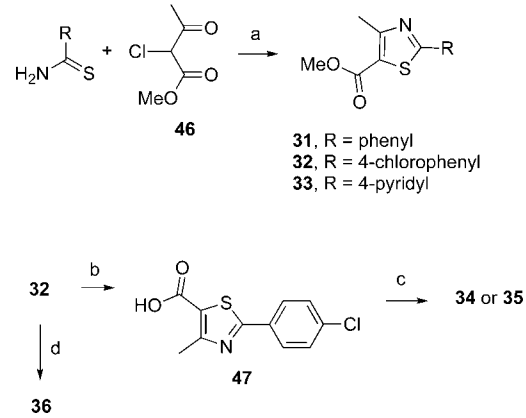

31, R = phenyl
32, R = 4-chlorophenyl
33, R = 4-pyridyl

[a] Reagents and conditions: (a) ethanol, heat to reflux for 2 h, 65−85%; (b) LiOH, methanol, ethanol, water, heated to reflux for 1 h, 80%; (c) 3,4-dichlorobenzylamine for **34** or adamantan-1-yl-methanol for **35**, EDCI, pyridine, RT for 12 h, 60%; (d) NBS, AIBN, CCl_4, heated to reflux for 12 h, 60%.

nonbonded interactions obtained from this extra binding may result in stronger biological activity.

Conclusion

Although the active compounds have variable structures, many of them share the common feature of a central thiazole ring. SAR analysis suggests that the hits **M02**, **P02**, and **D03** indeed provide promising structural templates for potential antiflaviviral agents. Replacing the Michael acceptor in **M02** with an amide in compound **11** significantly enhanced antiviral activity and diminished the undesired cytotoxicity. Alteration of the chloro and amino substitution pattern of the lead compound **D03** provided equally potent derivatives **23**−**27**.

The biological testing results indicate that compounds **11** and **36** inhibit yellow fever virus replication with EC_{50} values in the low micromolar range. Clearly, the preliminary antiviral potency displayed by these thiazole derivatives warrants further investigation. Future work will focus on modification of two

Table 1. Antiviral Activities vs Yellow Fever Virus and Cytotoxicities of the Original Hits and Second Generation Compounds

compound	EC_{50} (μM)[a]	CC_{50} (μM)[b]	TI[c]
M02	51 ± 7.2	70 ± 12	1.37
P02	13 ± 3	398 ± 0.1	30.6
D03	31 ± 0.3	61 ± 3	2.0
1	>50		
2	37.6 ± 2.8	154 ± 27	4.1
3	13.9 ± 1.5	155 ± 50	11.2
4	>50		
5	>50		
6	>50		
7	>50		
8	37.0 ± 7.0	138 ± 25	3.7
9	>50		
10	>50		
11	5 ± 1.7	186 ± 6	37
12	>50		
13	>50		
14	>50		
15	>50		
16	>50		
17	44 ± 5	123 ± 48	2.8
18	25 ± 4	200 ± 26	8
19	>50		
20	>50		
21	>50		
22	>50		
23	29 ± 16	151 ± 5	5.2
24	46 ± 0.5	119 ± 14	2.6
25	37 ± 13	155 ± 15	4.2
26	40 ± 0.3	131 ± 15	3.2
27	46 ± 6	133 ± 2	2.9
28	>50		
29	>50		
30	>50		
31	>50		
32	>50		
33	>50		
34	>50		
35	>50		
36	0.9 ± 0.7	153 ± 35	170

[a] The EC_{50} is the concentration of the compound resulting in a 50% inhibition in virus production. [b] The CC_{50} is the concentration of the compound causing a 50% growth inhibition of uninfected BHK cells. [c] TI is the therapeutic index and is equal to CC_{50}/EC_{50}.

of these structural templates, as well as NMR and crystallographic studies of drug−receptor complexes, testing vs drug-resistant mutant viruses, and evaluation of efficacy in animal models. On the basis of the data in hand, there is every reason to hope that derivatives of **11** or **36** could be developed into therapeutically useful antiviral agents.

Experimental Section

Experimental procedures for the syntheses of compounds **12**−**16**, **23**−**31**, **33**, and **34**, including analytical data, are reported in Supporting Information. Proton (^{1}H NMR) and carbon (^{13}C NMR) spectra were recorded in $CDCl_3$ or DMSO-d_6 on a Bruker ARX-300 or on a Bruker AVANCE 500 spectrometer. The NMR solvents are specified individually for each compound. Chemical shifts are given in parts per million (ppm) on the delta (δ) scale. The solvent peak or the internal standard tetramethylsilane were used as reference values. For ^{1}H NMR: $CDCl_3$ = 7.27 ppm, TMS = 0.00 ppm. Multiplicities were recorded as s (singlet), d (doublet), t (triplet), and m (multiplet). All reagents and dry solvents were purchased from Aldrich. All reactions were conducted under argon or nitrogen atmosphere, unless otherwise specified.

(*E*)-2-(3-(4-(1-(2-Carbamoylhydrazono)-ethyl)-phenyl)-ureido)-*N*-(2,4-dichlorobenzyl)-4-methylthiazole-5-carboxamide (1). Semicarbazide hydrochloride salt (20 mg, 0.22 mmol) was added to ethanol (5 mL). Et_3N was added dropwise to this mixture until it became a clear solution. A solution of 2-(3-(4-acetylphenyl)-ureido)-*N*-(2,4-dichlorobenzyl)-4-methylthiazole-5-carboxamide (**7**) (100 mg, 0.21 mmol) in ethanol (5 mL) was added to the reaction solution followed by acetic acid (0.1 mL). The reaction mixture was heated to reflux for 6 h. The reaction mixture was allowed to cool to room temperature. After removal of solvent under reduced pressure, the resulting residue was washed with cold ethyl acetate (1 mL × 3) and then recrystallized from ethanol to provide the desired compound as a white solid (80 mg, 73%): mp 184−186 °C. ^{1}H NMR (500 MHz, DMSO-d_6): δ 9.51 (s, 1 H), 9.24 (s, 1 H), 8.50 (s, 1 H), 7.77 (d, J = 7.5 Hz, 2 H), 7.57 (s, 1 H), 7.46 (d, J = 7.5 Hz, 1 H), 7.40 (d, J = 7.5 Hz, 1 H), 7.32 (d, J = 7.5 Hz, 1 H), 6.46 (s, 2 H), 4.39 (d, J = 3.0 Hz, 2 H), 2.44 (s, 3 H), 2.12 (s, 3 H). ^{13}C NMR (125 MHz, DMSO-d_6): δ 162.3, 159.0, 157.7, 143.9, 139.2, 136.0, 133.1, 133.0, 132.4, 130.4, 128.7, 127.7, 127.0 × 2, 118.2 × 2, 40.5, 17.1, 13.4. IR (KBr) 3271, 2922, 2851, 1667, 1531, 1454, 1373, 1309, 1248, 1187 cm^{-1}. MS (ES−) calcd for $C_{22}H_{20}Cl_2N_7O_3S$ 532.08, found 532.06. Anal. ($C_{22}H_{21}Cl_2N_7O_3S\cdot 0.5H_2O$) C, H, N.

(*E*)-2-(3-(4-(1-(2-Carbamimidoylhydrazono)-ethyl)-phenyl)-ureido)-*N*-(2,4-dichlorobenzyl)-4-methylthiazole-5-carboxamide (2). Aminoguanidine hydrochloride salt (20 mg, 0.22 mmol), 2-(3-(4-acetylphenyl)-ureido)-*N*-(2,4-dichlorobenzyl)-4-methylthiazole-5-carboxamide (**7**) (100 mg, 0.21 mmol), and acetic acid (0.1 mL) were added to ethanol (5 mL). The reaction mixture was heated to reflux for 6 h and allowed to cool to room temperature. After removal of solvent under reduced pressure, the resulting residue was washed with cold ethyl acetate (1 mL × 3) and then recrystallized from ethanol to provide the desired compound as a white solid (69 mg, 67%): mp 132−134 °C. ^{1}H NMR (500 MHz, DMSO-d_6): δ 11.4 (s, 1 H), 10.72 (s, 1 H), 8.52 (s, 1 H), 7.90 (d, J = 9.0 Hz, 2 H), 7.89 (s, 4 H), 7.56 (d, J = 2.0 Hz, 1 H), 7.49 (d, J = 9.0 Hz, 2 H), 7.39 (d, J = 8.5 Hz, 1 H), 7.33 (d, J = 8.5 Hz, 1 H), 4.38 (d, J = 5.5 Hz, 2 H), 2.46 (s, 3 H), 2.30 (s, 3 H). ^{13}C NMR (125 MHz, DMSO-d_6): δ 162.4, 158.5, 156.5, 152.1, 151.4, 140.5, 136.0, 133.1, 132.4, 130.4, 128.8, 127.9 × 2, 127.6, 117.7 × 2, 117.4, 40.5, 17.2, 14.9. IR (KBr) 1329, 1270, 913, 700 cm^{-1}. MS (ES+) calcd for $C_{22}H_{23}Cl_2N_8O_2S$ 533.10, found 532.88. HRMS (ES+) calcd for $C_{22}H_{20}Cl_2N_7O_3S$ 533.1042, found 533.1040.

Methyl 2-(3-(4-Acetylphenyl)ureido)-4-methylthiazole-5-carboxylate (3). 1-(4-Isocyanatophenyl)ethanone (500 mg, 3.1 mmol) was added to a solution of methyl 2-amino-4-methylthiazole-5-carboxylate (**39**) (550 mg, 3.1 mmol) in pyridine (15 mL). The reaction mixture was stirred at room temperature for 12 h. The solid was filtered and washed with cold methanol (5 mL × 3) to provide the desired compound as a white solid (876 mg, 83%): mp 270−272 °C. ^{1}H NMR (300 MHz, DMSO-d_6): δ 9.45 (s, 1 H), 7.90 (d, J = 9.0 Hz, 2 H), 7.60 (d, J = 9.0 Hz, 2 H), 3.76 (s, 3 H), 2.52 (s, 3 H), 2.50 (s, 3 H). ^{13}C NMR (125 MHz, pyridine-d_5): δ 197.5, 164.7, 164.4, 155.9, 155.7, 145.7, 133.3, 131.3 × 2, 119.7 × 2, 114.5, 52.8, 27.5, 17.8. IR (KBr) 3330, 1714, 1684, 1659, 1540, 1317, 1255, 1186, 762, 667 cm^{-1}. MS (ES+) calcd for $C_{15}H_{16}N_3O_4S$ 334.36, found 334.93. Anal. ($C_{15}H_{15}N_3O_4S$) C, H, N.

2-[3-(4-Acetylphenyl)-ureido]-4-methylthiazole-5-carboxylic Acid (4). Sodium hydroxide (200 mg, 5 mmol) was added to a solution of methyl 2-(3-(4-acetylphenyl)ureido)-4-methylthiazole-5-carboxylate (**3**) (100 mg, 0.3 mmol) in methanol (5 mL) and ethanol (5 mL). The reaction mixture was heated to reflux for 3 h and allowed to cool to room temperature. After removal of solvent under reduced pressure, water (10 mL) was added to the residue. The solution was filtered and acidified to pH 2−3 with hydrochloric acid. The generated solid was filtered and washed with cold hexanes (1 mL × 3) to provided the desired compound as a white solid (60 mg, 62%): mp 232−234 °C. ^{1}H NMR (500 MHz, DMSO-d_6): δ 9.43 (s, 2 H), 7.90 (d, J = 8.5 Hz, 2 H), 7.60 (d, J = 8.5 Hz, 2 H), 2.49 (s, 3 H), 2.46 (s, 3 H). ^{13}C NMR (125 MHz, pyridine-d_5): δ 197.5, 166.6, 164.7, 156.1, 153.9, 145.9, 134.6, 131.3 × 2, 119.7 × 2, 116.9, 27.5, 17.6. IR (KBr) 3367, 1716, 1598, 1535, 1486, 1410, 1313, 1272, 1176, 752, 680 cm^{-1}. MS (ES−) calcd for $C_{14}H_{12}N_3O_4S$ 318.34, found 318.23. Anal. ($C_{14}H_{13}N_3O_4S\cdot 1.5H_2O$) C, H, N.

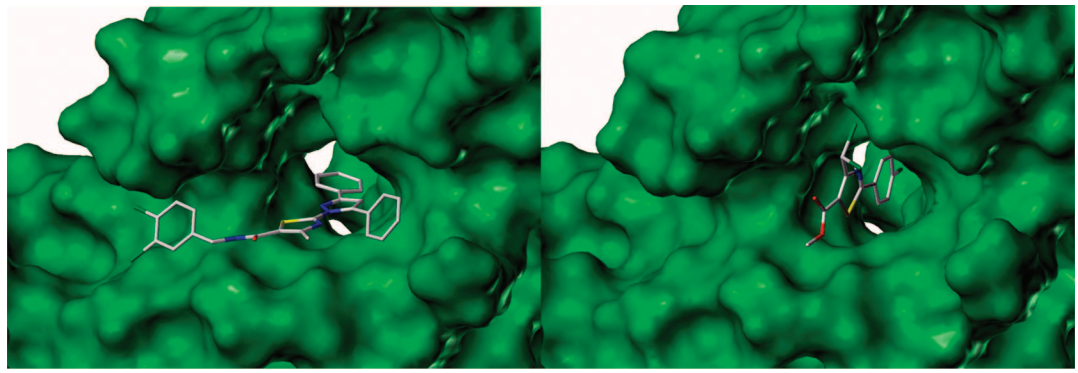

Figure 10. The docked models of compounds **11** (left) and **36** (right). The compounds are colored by atom type and the dengue β-OG binding pocket is displayed as a Connolly surface model.

(*E*)-Methyl 2-(3-(4-(1-(2-Carbamoylhydrazono)-ethyl)-phenyl)-ureido)-4-methylthiazole-5-carboxylate (5). Semicarbazide hydrochloride salt (111 mg, 1 mmol) was added to ethanol (5 mL). Et_3N was added dropwise to this mixture until it became a clear solution. A solution of methyl 2-(3-(4-acetylphenyl)ureido)-4-methylthiazole-5-carboxylate (**3**) (333 mg, 1 mmol) in ethanol (10 mL) was added to the reaction mixture, followed by acetic acid (0.5 mL). The reaction mixture was heated to reflux for 3 h and allowed to cool to room temperature. After removal of solvent under reduced pressure, the resulting residue was washed with cold ethyl acetate (1 mL × 3) and then recrystallized from ethanol to provide the desired compound as a white solid (323 mg, 83%): mp 265−267 °C. ^{1}H NMR (500 MHz, DMSO-d_6): δ 9.82 (s, 1 H), 9.21 (s, 1 H), 7.77 (d, J = 8.5 Hz, 2 H), 7.44 (d, J = 8.5 Hz, 2 H), 6.45 (s, 2 H), 3.72 (s, 3 H), 2.48 (s, 3 H), 2.11 (s, 3 H). ^{13}C NMR (125 MHz, DMSO-d_6): δ 162.9, 161.0, 157.7, 152.0, 144.3, 139.0, 133.1, 130.4, 127.0 × 2, 118.3 × 2, 117.9, 52.0, 17.2, 13.4. IR (KBr) 2382, 2300, 1698, 1535, 1493, 1376, 1328, 1259, 1219, 1070 cm^{-1}. MS (ES−) calcd for $C_{16}H_{17}N_6O_4S$ 389.11, found 388.98. Anal. calcd for $C_{16}H_{18}N_6O_4S\cdot 0.4H_2O$: C, 48.33; H, 4.77; N, 21.14. Found: C, 48.80; H, 4.70; N, 20.65.

(*E*)-Methyl 2-(3-(4-(1-(2-Carbamimidoylhydrazono)-ethyl)-phenyl)-ureido)-4-methylthiazole-5-carboxylate (6). Aminoguanidine hydrochloride salt (111 mg, 1 mmol) and methyl 2-(3-(4-acetylphenyl)ureido)-4-methylthiazole-5-carboxylate (**3**) (333 mg, 1 mmol) were added to ethanol (10 mL), followed by acetic acid (0.5 mL). The reaction solution was heated to reflux for 3 h and allowed to cool to room temperature. After removal of solvent under reduced pressure, the resulting residue was washed with cold ethyl acetate (1 mL × 3) and then recrystallized from ethanol to provide the desired compound as a white solid (291 mg, 75%): mp 212−214 °C. ^{1}H NMR (500 MHz, DMSO-d_6): δ 11.0 (s, 2 H), 10.4 (s, 1 H), 7.90 (d, J = 8.5 Hz, 2 H), 7.50 (d, J = 8.5 Hz, 2 H), 3.73 (s, 3 H), 2.49 (s, 3 H), 2.26 (3 H). IR (KBr) 2382, 1319 cm^{-1}. MS (ES+) calcd for $C_{16}H_{20}N_7O_3S$ 390.13, found 389.76. HRMS (ES+) calcd for $C_{16}H_{20}N_7O_3S$ 390.1348, found 390.1340. Anal. ($C_{16}H_{19}N_7O_3S\cdot 4$/3HCl) C, H, N.

2-(3-(4-Acetylphenyl)-ureido)-*N*-(2,4-dichlorobenzyl)-4-methylthiazole-5-carboxamide (7). 2,4-Dichlorobenzylamine (90 mg, 0.5 mmol) and EDCI (100 mg, 0.52 mmol) were added to a solution of 2-[3-(4-acetyl-phenyl)-ureido]-4-methyl-thiazole-5-carboxylic acid (**4**) (150 mg, 0.46 mmol) in pyridine (5 mL). The reaction mixture was stirred at room temperature overnight. After removal of solvent under reduced pressure, water (1 mL) was added to the residue. The resulting mixture was stirred for 1 h at room temperature. The solid was filtered and washed with cold methanol (1 mL × 3) to provide the desired compound as a white solid (138 mg, 63%): mp 214−216 °C. ^{1}H NMR (300 MHz, DMSO-d_6): δ 9.49 (s, 1 H), 8.54 (dd, J = 5.7, 5.7 Hz, 1 H), 7.92 (d, J = 8.4 Hz, 2 H), 7.63 (d, J = 8.4 Hz, 2 H), 7.43 (d, J = 8.4 Hz, 1 H), 7.35 (d, J = 8.4 Hz, 1 H), 4.41 (d, J = 5.7 Hz, 2 H), 2.52 (s, 3 H), 2.47 (s, 3 H). ^{13}C NMR (125 MHz, pyridine-d_5): δ 197.5, 164.3, 163.1, 156.1, 145.6, 136.9, 135.9, 134.7, 134.0, 132.8, 131.3, 130.9 × 2, 130.2, 128.3, 119.7 × 2, 117.6, 42.1, 27.1, 17.4. IR (KBr) 3246, 1537, 1176 cm^{-1}. MS (ES−) calcd for $C_{21}H_{17}Cl_2N_4O_3S$ 475.05, found 474.95. Anal. ($C_{21}H_{18}Cl_2N_4O_3S\cdot 2/3H_2O$) C, H, N.

2-(3-(4-Acetylphenyl)-ureido)-*N*-(3,4-dichlorobenzyl)-4-methylthiazole-5-carboxamide (8). 3,4-Dichlorobenzylamine (90 mg, 0.5 mmol) and EDCI (100 mg, 0.52 mmol) were added to a solution of 2-[3-(4-acetyl-phenyl)-ureido]-4-methyl-thiazole-5-carboxylic acid (**4**) (150 mg, 0.46 mmol) in pyridine (5 mL). The reaction mixture was stirred at room temperature overnight. After removal of solvent under reduced pressure, the resulting residue was purified by chromatography (ethyl acetate−hexanes = 2:3) to provide the desired compound as a white solid (153 mg, 70%): mp 262−264 °C. ^{1}H NMR (300 MHz, DMSO-d_6): δ 9.53 (s, 1 H), 8.57 (dd, J = 5.7, 5.7 Hz, 1 H), 7.93 (d, J = 8.7 Hz, 2 H), 7.63 (d, J = 8.7 Hz, 2 H), 7.60 (d, J = 8.4 Hz, 1 H), 7.55 (d, J = 1.8 Hz, 1 H), 7.30 (dd, J = 8.4, 1.8 Hz, 1 H), 4.36 (d, J = 6.0 Hz, 2 H), 2.52 (s, 3 H), 2.50 (s, 3 H). ^{13}C NMR (75 MHz, DMSO-d_6): δ 197.3, 162.7, 141.9, 133.1, 132.4, 131.7, 131.4, 130.6 × 2, 133.0, 130.2, 130.1, 128.6, 118.6 × 2, 42.6, 27.3, 17.4. IR (KBr) 3252, 1534, 1177 cm^{-1}. MS (ES+) calcd for $C_{21}H_{19}Cl_2N_4O_3S$ 477.05, found 477.0. Anal. ($C_{21}H_{18}C_{12}N_4O_3S\cdot 1.5\ H_2O$) C, H, N.

Ethyl 2-(3,5-Diphenyl-1*H*-pyrazol-1-yl)-4-methylthiazole-5-carboxylate (9). 3,5-Diphenyl-1*H*-pyrazole (**17**) (80 mg, 0.4 mmol), 2-bromo-4-methyl-thiazole-5-carboxylic acid ethyl ester (**40**) (125 mg, 0.5 mmol), Cu_2O (10 mg, 0.07 mmol), and 2-hydroxybenzaldehyde oxime (10 mg, 0.07 mmol) were added to a solution of cesium carbonate (325 mg, 1 mmol) in predegassed anhydrous CH_3CN (5 mL) in a pressure reaction vessel. Argon gas was induced into the reaction mixture for 20 min. Then the vessel was sealed with a cap. The reaction mixture was heated to 80−90 °C for 8 h. After removal of solvent under reduced pressure, the residue was dissolved in methanol and purified by chromatography (ethyl acetate−hexanes = 1:9) to provide the desired compound as a white solid (100 mg, 65%): mp 114−116 °C. ^{1}H NMR (300 MHz, $CDCl_3$): δ 7.92 (d, J = 6.9 Hz, 2 H), 7.55 (m, 2 H), 7.44 (m, 6 H), 6.79 (s, 1 H), 4.31 (ddd, J = 6.9, 6.9, 6.9 Hz, 2 H), 2.51 (s, 3 H), 1.34 (dd, J = 7.2, 7.2 Hz, 3 H). ^{13}C NMR (75 MHz, $CDCl_3$): δ 162.1, 162.0, 158.2, 153.8, 145.9, 131.4, 129.6 × 2, 129.5, 129.0, 128.9, 128.6 × 2, 127.7 × 2, 126.0 × 2, 119.2, 108.4, 61.0, 17.4, 14.2. IR (KBr) 1712, 1499, 1256, 1095, 759 cm^{-1}. MS (ES+) calcd for $C_{22}H_{20}N_3O_2S$ 390.12, found 390.12. Anal. ($C_{22}H_{19}N_3O_2S$) C, H, N.

2-(3,5-Diphenyl-1*H*-pyrazol-1-yl)-4-methylthiazole-5-carboxylic Acid (10). Lithium hydroxide (120 mg, 5 mmol) was added to a solution of ethyl 2-(3,5-diphenyl-1*H*-pyrazol-1-yl)-4-methylthiazole-5-carboxylate (**9**) (70 mg, 0.18 mmol) in methanol (5 mL), ethanol (10 mL), and water (5 mL). The reaction mixture was heated to reflux for 3 h. After removal of solvent under reduced pressure, the residue was dissolved in water (10 mL) and the resulting solution was filtered. The solution was acidified to pH 2−3 with hydrochloric acid and the resulting solid was filtered. The crude product was recrystallized from methanol (10 mL) to provide the desired compound as a white solid (51 mg, 80%): mp 232−234

°C. ^{1}H NMR (500 MHz, DMSO-d_6): δ 7.93 (d, J = 7.5 Hz, 2 H), 7.57 (br, s, 2 H), 7.48 (m, 6 H), 7.23 (s, 1 H), 2.35 (s, 3 H). ^{13}C NMR (75 MHz, $CDCl_3$): δ 163.7, 161.9, 157.4, 154.2, 146.6, 131.8, 130.4 × 2, 130.2, 130.1, 129.8 × 2, 128.7 × 2, 126.8 × 2, 126.0, 121.3, 110.0, 17.4. IR (KBr) 2925, 1675, 1493, 1316, 759 cm^{-1}. MS (ES−) calcd for $C_{20}H_{14}N_3O_2S$ 360.09, found 359.87. Anal. ($C_{22}H_{15}N_3O_2S \cdot 2.17H_2O$) C, H, N.

***N*-(3,4-Dichlorobenzyl)-2-(3,5-diphenyl-1*H*-pyrazol-1-yl)-4-methylthiazole-5-carboxamide (11).** 3,4-Dichlorobenzylamine (25 mg, 0.13 mmol) was added to a solution of 2-(3,5-diphenyl-1*H*-pyrazol-1-yl)-4-methylthiazole-5-carboxylic acid (**10**) (45 mg, 0.125 mmol) in anhydrous pyridine (3 mL). EDCI (20 mg, 0.13 mmol) was added to the resulting solution. The reaction mixture was stirred at room temperature overnight. After removal of solvent under reduced pressure, the resulting residue was purified by silica gel chromatography (ethyl acetate−hexanes = 1:4) to provide the desired compound as a white solid (47 mg, 70%): mp 144−146 °C. ^{1}H NMR (500 MHz, $CDCl_3$): δ 7.90 (d, J = 7.5 Hz, 2 H), 7.53 (d, J = 7.5 Hz, 2 H), 7.43 (m, 8 H), 7.18 (dd, J = 8.5, 2.0 Hz, 1 H), 6.79 (s, 1 H), 6.04 (dd, J = 6.0, 6.0 Hz, 1 H), 4.55 (d, J = 6.0 Hz, 2 H), 2.48 (s, 3 H). IR (KBr) 2994, 1770, 1056, 744 cm^{-1}. MS (ES+) calcd for $C_{27}H_{21}Cl_2N_4OS$ 519.07, found 518.95. HRMS (ES+) calcd for $C_{27}H_{20}Cl_2N_4OSNa$ 541.0633, found 541.0636. Anal. ($C_{27}H_{20}Cl_2N_4OS$) C, H, N.

Methyl 2-(Bis(4-acetylbenzyl)amino)-4-methylthiazole-5-carboxylate (18). Sodium hydride (95%, 30 mg, 1 mmol) was added to a solution of methyl 2-amino-4-methylthiazole-5-carboxylate **(39)** (86 mg, 0.5 mmol) in anhydrous DMF (5 mL) at 0 °C under argon gas. The reaction mixture was stirred for 1 h until it became a clear solution. 1-(4-(Bromomethyl)phenyl)ethanone (**41**) (211 mg, 1 mmol) was added to this solution and the resulting mixture was stirred at 0 °C for 1 h and at room temperature for additional 3 h. Ice water (10 mL) was added to the reaction mixture. The resulting solution was extracted with ethyl acetate (10 mL × 3). The organic layer was concentrated under reduced pressure. The residue was purified by silica gel chromatography (ethyl acetate−hexanes = 1:4) to provide the desired compound as a white solid (260 mg, 74%): mp 162−164 °C. ^{1}H NMR (500 MHz, $CDCl_3$): δ 7.92 (d, J = 8.1 Hz, 4 H), 7.31 (d, J = 8.1 Hz, 4 H), 4.73 (s, 4 H), 3.78 (s, 3 H), 2.60 (s, 9 H). ^{13}C NMR (125 MHz, $CDCl_3$): δ 197.4 × 2, 171.1, 162.8, 160.2, 140.7 × 2, 136.7 × 2, 128.9 × 4, 127.7 × 4, 109.9, 53.4 × 2, 51.4, 26.5 × 2, 17.5. IR (KBr) 2949, 1682, 1525, 1265, 1094 cm^{-1}. MS (ES+) calcd for $C_{24}H_{25}N_2O_4S$ 437.15, found 437.00. Anal. ($C_{24}H_{25}N_2O_4S$) C, H, N.

2-(Bis(4-acetylbenzyl)amino)-*N*-(2,4-dichlorobenzyl)-4-methylthiazole-5-carboxamide (19). 2,4-Dichlorobenzylamine (86 mg, 0.5 mmol) was added to a solution of 2-(bis(4-acetylbenzyl)amino)-4-methylthiazole-5-carboxylic acid (**42**) (210 mg, 0.5 mmol) in anhydrous pyridine (10 mL). EDCI (100 mg, 0.6 mmol) was added to the resulting solution. The reaction mixture was stirred at room temperature overnight. After removal of solvent under reduced pressure, the resulting residue was purified by silica gel chromatography (ethyl acetate−hexanes = 1:4) to provide the desired compound as a colorless oil (210 mg, 72%). ^{1}H NMR (300 MHz, $CDCl_3$): δ 7.90 (d, J = 8.1 Hz, 4 H), 7.37 (d, J = 8.5 Hz, 1 H), 7.36 (s, 1 H), 7.30 (d, J = 8.1 Hz, 4 H), 7.20 (m, 1 H), 6.01 (dd, J = 6.3, 6.3 Hz, 1 H), 4.69 (s, 4 H), 4.57 (d, J = 6.3 Hz, 2 H), 2.59 (s, 6 H), 2.54 (s, 3 H). ^{13}C NMR (75 MHz, $CDCl_3$): δ 197.4 × 2, 169.2, 162.8, 160.0, 154.0, 140.9 × 2, 136.5 × 2, 131.2, 129.2, 128.5, 127.4, 128.8 × 4, 127.6 × 4, 127.3, 10.9, 53.3 × 2, 41.2, 26.5 × 2, 17.8. IR (KBr) 3375, 1682, 1521, 1267 cm^{-1}. MS (ES+) calcd for $C_{30}H_{28}Cl_2N3O_3S$ 580.12, found 580.07. Anal. ($C_{30}H_{27}Cl_2N_3O_3S$) C, H, N.

Methyl 2-(*N*-(4-Acetylbenzyl)acetamido)-4-methylthiazole-5-carboxylate (20). Sodium hydride (500 mg, 22 mmol) was added to a solution of methyl 2-amino-4-methylthiazole-5-carboxylate (**39**) (1.7 g, 10 mmol) in DMF (20 mL). The reaction mixture was stirred at 0 °C for 30 min. A solution of 1-(4-(bromomethyl)phenyl)ethanone (**41**) (4.2 g, 20 mmol) in ethyl acetate (5 mL) was slowly added to the reaction mixture. The reaction mixture was stirred at room temperature for 4 h. After removal of solvent under reduced pressure, the reaction residue was poured into water (5 mL). The generated solids were filtered, washed with cold hexanes (1 mL × 3), and recrystallized from methanol (10 mL) to provide the desired compound as yellow solid (2.4 g, 70%): mp 182−184 °C. ^{1}H NMR (300 MHz, $CDCl_3$): δ 7.92 (d, J = 8.1 Hz, 2 H), 7.26 (d, J = 8.0 Hz, 2 H), 5.55 (s, 2 H), 3.85 (s, 3 H), 2.58 (s, 6 H), 2.03 (s, 3 H). ^{13}C NMR (75 MHz, $CDCl_3$): δ 197.3, 170.5, 163.6, 160.4, 155.9, 141.4, 136.5, 128.9 × 2, 126.2 × 2, 116.8, 51.6, 50.4, 26.5, 22.9, 17.3. IR (KBr) 3375, 1682, 1643, 1507, 1437, 1100 cm^{-1}. MS (ES+) calcd for $C_{17}H_{19}N_2O_4S$ 347.10, found 347.01. Anal. ($C_{17}H_{19}N_2O_4S \cdot 0.5H_2O$) C, H, N.

2-(4-Chlorophenyl)-4-methylthiazole (21). 4-Chlorobenzothioamide (**43**) (170 mg, 1 mmol) was added to a solution of 1-chloroacetone (**44**, 360 mg, 4 mmol) in absolute ethanol (5 mL). The reaction mixture was heated to reflux for 2 h. After removal of solvent under reduced pressure, the residue was purified by silica gel chromatography (ethyl acetate−hexanes = 1:4) to provide the desired compound as a white solid (167 mg, 80%): mp 128−130 °C. ^{1}H NMR (500 MHz, $CDCl_3$): δ 8.30 (d, J = 8.7 Hz, 2 H), 7.53 (d, J = 8.7 Hz, 2 H), 7.22 (s, 1 H), 2.79 (s, 3 H). ^{13}C NMR (125 MHz, $CDCl_3$): δ 169.4, 148.4, 140.3, 130.1 × 2, 129.5 × 2, 124.8, 115.2, 14.4. IR (KBr) 1598, 1093, 1003, 831, 750, 697 cm^{-1}. MS (ES+) calcd for $C_{10}H_9ClNS$ 210.01, found 210.03. Anal. calcd for $C_{10}H_8ClNS \cdot 2H_2O$: C, 48.88; H, 4.92; N, 5.70. Found: C, 48.46; H, 4.38; N, 5.25.

4-(Chloromethyl)-2-(4-chlorophenyl)thiazole (22). 4-Chlorobenzothioamide (350 mg, 2.0 mmol) was added to a solution of 1,3-dichloroacetone (**45**) (500 mg, 4.0 mmol) in absolute ethanol (10 mL). The reaction mixture was heated to reflux for 2 h. After removal of solvent under reduced pressure, the residue was recrystallized from hexanes to provide the desired compound as a white solid (315 mg, 65%): mp 74−76 °C. ^{1}H NMR (500 MHz, $CDCl_3$): δ 7.88 (d, J = 8.5 Hz, 2 H), 7.42 (d, J = 8.5 Hz, 2 H), 7.31 (s, 1 H), 4.74 (s, 2 H). ^{13}C NMR (125 MHz, $CDCl_3$): δ 167.8, 153.3, 136.3, 131.6, 129.1 × 2, 127.7 × 2, 117.4, 40.8 (d). IR (KBr) 3374, 3107, 2917, 1656, 1497, 1453, 1398, 1262, 1244, 1104, 1091, 1038, 838, 722, 652 cm^{-1}. MS (ES+) calcd for $C_{10}H_8Cl_2NS$ 243.97, found 243.89. Anal. ($C_{10}H_7Cl_2NS \cdot 1/3H_2O$) C, H, N.

2-((2-(4-Chlorophenyl)thiazol-4-yl)methylthio)aniline (D03). $CsCO_3$ (160 mg, 0.50 mmol) was added to a solution of 2-aminobenzenethiol (40 mg, 0.33 mmol) in anhydrous DMF (5 mL) at 0 °C under argon. Argon gas was bubbled through the reaction mixture for 30 min. Then the reaction mixture was allowed to warm to room temperature. 4-(Chloromethyl)-2-(4-chlorophenyl)thiazole (**22**) (80 mg, 0.33 mmol) was added to the reaction mixture, and the resulting mixture was stirred at room temperature for 0.5 h. The reaction mixture was heated to reflux for additional 2 h and allowed to cool to room temperature. After removal of solvent under reduced pressure, the resulting residue was purified by silica gel chromatography (ethyl acetate−hexanes = 1:9) to provide the desired compound as a colorless oil (76 mg, 70%). ^{1}H NMR (500 MHz, $CDCl_3$): δ 7.86 (d, J = 8.5 Hz, 2 H), 7.40 (d, J = 8.5 Hz, 2 H), 7.25 (m, 1 H), 7.11 (ddd, J = 7.5, 7.5, 0.5 Hz, 1 H), 6.75 (s, 1 H), 6.69 (dd, J = 7.5, 0.5 Hz, 1 H), 6.65 (ddd, J = 7.5, 7.5, 0.5 Hz, 1 H), 4.38 (br, s, 2 H), 4.06 (s, 2 H). ^{13}C NMR (125 MHz, $CDCl_3$): δ 166.8, 154.3, 148.6, 136.7, 136.0, 131.7, 130.2, 129.0 × 2, 127.6 × 2, 118.2, 116.9, 115.7, 114.7, 34.8. IR (KBr) 2922, 1606, 1478, 1219, 1091, 831 cm^{-1}. MS (ES+) calcd for $C_{16}H_{14}ClN_2S_2$ 333.02, found 332.95. Anal. ($C_{16}H_{13}ClN_2S_2$) C, H, N.

2-(4-Chlorophenyl)-4-methyl-thiazole-5-carboxylic Acid Methyl Ester (32). 4-Chloro-thiobenzamide (51 mg, 0.3 mmol) and 2-chloro-3-oxo-butyric acid methyl ester (**46**, 45 mg, 0.3 mmol) were added to absolute ethanol (5 mL). The reaction mixture was heated to reflux for 2 h. After removal of solvent under reduced pressure, the residue was purified by silica gel chromatography (ethyl acetate−hexanes = 1:9) to provide the desired compound as a white solid (60 g, 75%): mp 130−132 °C. ^{1}H NMR (500 MHz, $CDCl_3$): δ 7.89 (d, J = 8.5 Hz, 2 H), 7.41 (d, J = 8.5 Hz, 2 H), 3.89 (s, 3 H), 2.77 (s, 3 H). ^{13}C NMR (125 MHz, $CDCl_3$): δ 168.4, 162.4, 161.2, 136.9, 131.2, 129.1 × 2, 127.9 × 2, 121.5, 52.1, 17.4.

IR (KBr) 1717, 1519, 1435, 1398, 1328, 1277, 1090, 830, 758 cm^{-1}. MS (ES+) calcd for $C_{12}H_{11}ClNO_2S$ 268.01, found 267.92. Anal. ($C_{12}H_{10}ClNO_2S$) C, H, N.

2-(4-Chloro-phenyl)-4-methyl-thiazole-5-carboxylic Acid Adamantan-1-ylmethyl Ester (35). 2-(4-Chloro-phenyl)-4-methyl-thiazole-5-carboxylic acid methyl ester (**32**, 80 mg, 0.3 mmol) and LiOH (45 mg, 1.8 mmol) were added to ethanol−methanol−H_2O (3 mL, 1:1:1). The reaction mixture was heated at reflux for 1 h and allowed to cool to room temperature. The reaction mixture was filtered. After removal of solvent under reduced pressure, water (5 mL) was added. After adjusting pH to 3−4 with HCl, the solid was filtered and washed with water and a small amount of ethanol. The solid was dried to provide 2-(4-chloro-phenyl)-4-methyl-thiazole-5-carboxylic acid as a white solid (**47**, 60 mg, 80%) that was used directly in the next step without further purification. 2-(4-Chlorophenyl)-4-methyl-thiazole-5-carboxylic acid (**47**, 60 mg, 0.25 mmol) and EDCI (50 mg, 0.25 mmol) and adamantan-1-yl-methanol (40 mg, 0.25 mmol) were added to pyridine (5 mL). The reaction mixture was stirred at room temperature for 12 h. After removal of solvent under reduced pressure, water (5 mL) was added. The obtained solution was extracted by ethyl acetate (2 mL × 3). The organic layer was washed by brine (1 mL × 3). After removal of solvent under reduced pressure, the residue was purified by silica gel chromatography (ethyl acetate−hexanes = 1:9) to provide the desired compound as a colorless oil (60 mg, 60%). ^{1}H NMR (300 MHz, $CDCl_3$): δ 7.93 (d, J = 8.7 Hz, 2 H), 7.43 (d, J = 8.7 Hz, 2 H), 3.89 (s, 2 H), 2.79 (s, 3 H), 2.02 (s, 3 H), 1.70 (m, 12 H). ^{13}C NMR (75 MHz, $CDCl_3$): δ 168.4, 162.2, 160.8, 136.9, 131.3, 129.2 × 2, 127.9 × 2, 122.2, 74.7, 39.2, 36.8, 33.2, 29.6, 27.9, 17.5, 0.9. IR (KBr) 2903, 2848, 1714, 1437, 1260, 1092 cm^{-1}. MS (ES+) calcd for $C_{22}H_{25}ClNO_2S$ 402.12, found 402.02. Anal. ($C_{22}H_{24}ClNO_2S$) C, H, N.

2-(4-Chloro-phenyl)-4-dibromomethyl-thiazole-5-carboxylic Acid Methyl Ester (36). 2-(4-Chlorophenyl)-4-methyl-thiazole-5-carboxylic acid methyl ester (**32**, 133 mg, 0.5 mmol) and NBS (531 mg, 3 mmol) were added to CCl_4 (10 mL). The reaction mixture was heated at reflux for 12 h. After removal of solvent under reduced pressure, the residue was purified by silica gel chromatography (ethyl acetate−hexanes = 1:4) to provide the desired compound as a white solid (127 mg, 60%): mp 154−156 °C. ^{1}H NMR (300 MHz, $CDCl_3$)L δ 7.96 (d, J = 8.5 Hz, 2 H), 7.69 (s, 1 H), 7.44 (d, J = 8.5 Hz, 2 H), 3.94 (s, 3 H). ^{13}C NMR (75 MHz, $CDCl_3$): δ 170.0, 160.8, 158.8, 137.8, 130.5, 129.3 × 2, 128.2 × 2, 120.0, 52.9, 31.0. IR (KBr) 3044, 1714, 1514, 1447, 1287, 1091, 833, 719, 623 cm^{-1}. Anal. ($C_{12}H_8Br_2ClNO_2S$) C, H, N.

Methyl 2-Bromo-3-oxobutanoate (38). NBS (18 g, 110 mmol) and a catalytic amount of AIBN were added to a solution of methyl 3-oxobutanoate (**37**) (12 g, 100 mmol) in anhydrous benzene (50 mL). The reaction mixture was stirred at room temperature for 2 h. After removal of solvent under reduced pressure, the residue was purified by silica gel chromatography (ethyl acetate−hexanes = 2:3) to provide the desired compound as a colorless oil (20 g, 100%). ^{1}H NMR (300 MHz, $CDCl_3$): δ 4.73 (s, 1 H), 3.37 (s, 3 H), 2.38 (s, 3 H).

Methyl 2-Amino-4-methylthiazole-5-carboxylate (39). Thiourea (4 g, 50 mmol) was added to a solution of methyl 2-bromo-3-oxobutanoate (**38**, 10 g, 50 mmol) in ethanol (100 mL). The reaction mixture was stirred at room temperature for 3 h. After removal of the solvent under reduced pressure, the crude product was recrystallized from fresh ethyl acetate (30 mL) and methanol (15 mL). The solid was filtered and washed with diethyl ether to provide the desired compound as a white solid (7 g, 81%): mp 132−134 °C. ^{1}H NMR (300 MHz, DMSO-d_6): δ 3.57 (s, 3 H), 2.26 (s, 3 H); MS (ES+) calcd for $C_6H_9N_2O_2S$ 173.03, found 172.95.

2-(Bis(4-acetylbenzyl)amino)-4-methylthiazole-5-carboxylic Acid (42). Sodium hydroxide (200 mg, 5 mmol) was added to a solution of methyl 2-(*N*-(4-acetylbenzyl)acetamido)-4-methylthiazole-5-carboxylate (**18**, 100 mg, 0.23 mmol) in methanol (5 mL) and ethanol (5 mL). The reaction mixture was heated to reflux for 1 h and allowed to cool to room temperature. After removal of solvent under reduced pressure, water (5 mL) was added to the residue. The pH was adjusted to 2−3 with hydrochloric acid. The generated solid was filtered and washed with cold hexanes (1 mL × 3) to provide the desired compound as an off-white solid (67 mg, 70%): mp 75−77 °C. ^{1}H NMR (300 MHz, DMSO-d_6): δ 7.92 (d, J = 8.0 Hz, 4 H), 7.30 (d, J = 8.0 Hz, 4 H), 4.72 (br, s, 4 H), 2.60 (s, 9 H); MS (ES+) calcd for $C_{23}H_{22}N_2O_4S$ 422.13, found 422.86.

2-Chloro-3-oxo-butyric Acid Methyl Ester (46). Sufuryl chloride (18 g, 110 mmol) and a catalytic amount of AIBN were added to a solution of methyl 3-oxobutanoate (12 g, 100 mmol) in anhydrous benzene (50 mL). The reaction mixture was stirred at room temperature for 2 h. After removal of solvent under reduced pressure, the residue was purified by silica gel chromatography (ethyl acetate−hexanes = 2:3) to provide the desired compound as a colorless oil (20 g, 100%). ^{1}H NMR (300 MHz, $CDCl_3$): δ 4.73 (s, 1 H), 3.37 (s, 3 H), 2.38 (s, 3 H).

Molecular Modeling. Compounds **1**−**36** were built within Sybyl 7.1 and minimized to 0.01 kcal/mol by the Powell method, using Gasteiger−Huckel charges and the Tripos force field. To save calculation time, solvent was not explicitly included and instead the dielectric constant was set to a value of 4. The minimized molecules underwent 10 rounds of simulated annealing to further relax the conformations of these manually drawn molecules. Conformations resulting from each simulation were selected and the energies were minimized using the same parameter set as the one used during molecule construction. The conformer with the lowest energy was used as the initial structure for each molecule to be docked into the β-OG binding pocket of the dengue virus E protein.

Docking Simulation. The energy-optimized compounds were docked into the β-OG binding domain in E protein of the dengue virus that was obtained by removal of the *n*-octyl-β-D-glucoside (BOG). The parameters were set as the default value that the GOLD software suggested.

Bioassay Methods. BHK cells. BHK-15 cells (baby hamster kidney cells) obtained from the American Type Culture Collection (ATCC, Rockville, MD) were maintained in minimal essential medium (MEM) (Invitrogen, Carlsbad, CA) containing 7.5% fetal bovine serum (FBS). Cells were grown in incubators at 37 °C in the presence of 5% CO_2.

YFV-IRES-Luc. A fire-fly luciferase reporter gene was inserted into pYF23, a derivative of pACNR, which is the full-length cDNA clone of YFV 17D, to construct YFV-IRES-Luc, a luciferase-reporting full-length virus. To facilitate this construction, an NsiI restriction site was introduced at the beginning of the 3′ NTR immediately following the UGA termination codon of NS5 in pYF23 using standard overlapping PCR mutagenesis. To construct YFV-IRES-Luc, an IRES-FF-Luc (EMCV IRES-fire fly luciferase) cassette was amplified by PCR from YFRP-IRES-Luc, a YFV replicon, and inserted into the NsiI restriction site.

Generation of YFV-IRES-Luc Virus. In vitro transcribed YFV-IRES-Luc RNA was transfected into BHK-15 cells via electroporation. Subconfluent monolayers of cells were grown in T-75 culture flasks and were harvested by trypsinization, then subsequently washed twice with phosphate-buffered saline (PBS) before being resuspended in 400 μL PBS. These cells were then combined with 40 μL of in vitro transcribed RNA, and then placed in a 2-mm gap cuvette (BioRad, Hercules, CA). The cells were subjected to electroporation by being pulsed two times at settings of 1.5 kV, 25 μF, and 200 Ω using a GenePulser II apparatus (BioRad). After the two pulses, the cells were given a 5 min recovery time at room temperature. Following recovery, cells were resuspended in MEM supplemented with 10% FBS. At 4 days post-transfection, the resulting YFV-IRES-Luc virus was harvested and the titer of the virus determined by a standard plaque assay. The infectivity of the virus could be assayed directly as a measure of the luciferase amounts produced in infected cells over a period of time.

Inhibition of YFV-IRES-Luc Virus Growth. BHK cells were plated in a 96-well plate and grown at 37 °C. At confluency, cells were infected with YF-IRES-Luc virus[32] at a multiplicity of infection (MOI) of 0.1. A low MOI was utilized to ensure that

fewer cells were infected so that the spread of released virus could be monitored. Cells were then overlaid with culture media containing serial dilutions of compounds at concentrations below the CC_{50} values. Controls included uninfected cells, infected cells, and DMSO-treated infected cells. Cells were incubated at 37 °C, 5% CO_2 for ~36 h, lysed using 50 μL of cell culture lysis buffer (Promega Inc., Madison, WI), and 20 μL of cell extracts were placed into a 96-well opaque plate. Luciferase activity was determined from the luminescence generated with fire-fly luciferase substrate (Promega Inc., Madison, WI). Luminescence was measured in a 96-well plate luminometer, LMax II (Molecular Devices, Sunnyvale, CA). A reduction in luciferase activity indicates inhibition of YFV-IRES-Luc virus growth. The luciferase luminescence as a function of compound concentration was analyzed by nonlinear regression analysis using GraphPad Prizm to estimate the EC_{50} of each compound. The EC_{50} was defined as the concentration of the compound to cause 50% reduction of luciferase activity in infected cells as compared to the DMSO treated cells.

Dengue Immunofluorescence Assay. In brief, Den-2 (strain 16681) was added to monolayers of BHK cells in a 24-well plate at an moi of 0.025 for 1 h at room temperature. Following infection, the excess/unbound virus was removed by washing with PBS. Cells were then overlaid with MEM + 2.5% FBS containing the compound at 50 μM concentration. The cells were then incubated at 34 °C for 48 h before performing immunofluorescence assay. Cell monolayers were fixed and incubated with the antidengue capsid antibody for 2 h, followed by incubation with the secondary antibody conjugated with TRITC. Three randomly selected fields per well were captured in both the TRITC (tetramethylrhodamine-5 (and 6)-isothiocyanate) and DAPI (4′,6-diamidino-2-phenylindole dihydrochloride) channels. All infected cells were compared to total cells in all three fields and percent inhibition was determined.

Cell Viability Assay. Cellular viability was measured spectrophotometrically by monitoring the reduction of a tetrazolium salt to a formazan dye by mitochondrial dehydrogenase in living cells. BHK cells were plated in a 96-well plate and grown at 37 °C. At confluency, cells were overlaid with culture media containing serial dilutions of compounds (compound stocks were generated by dissolving compounds in DMSO). Untreated and DMSO treated cells served as positive controls. Cells were then incubated at 37 °C, 5% CO_2 for ~36 h. At ~36 h post-treatment, media on cells was replaced with fresh media to remove the compounds. Then 100 μL of XTT-substrate from the Quick Cell Proliferation Kit (Biovision Inc., CA) was added to each well. Cells were incubated at 37 °C for a further 2 h. Plates were then removed and OD_{450} measured using a 96-well plate reader (Molecular Devices, Sunnyvale, CA). The OD_{450} values for cells treated with a compound were compared to those obtained for cells treated with the control (1% DMSO) to determine the CC_{50} of each compound. The 1% DMSO in the control was necessary to solubilize some of the compounds, and it did not affect cell viability.

Acknowledgment. This work was sponsored by the NIH/NIAID Regional Center of Excellence for Biodefense and Emerging Infectious Diseases Research (RCE) Program. We wish to acknowledge membership within and support from the Region V "Great Lakes" RCE (NIH award 1-U54-AI-057153). This research was conducted in a facility constructed with support from Research Facilities Improvement Program grant number C06-14499 from the National Center for Research Resources of the National Institutes of Health. We are grateful to Dr. Huaping Mo for assistance with NMR spectroscopy.

Supporting Information Available: Results from elemental analyses of intermediates and target compounds, and full experimental details, including spectral data, for the syntheses of compounds **12**−**16**, **23**−**31**, **33**, and **34**. This material is available free of charge via the Internet at http://pubs.acs.org.

References

(1) Cheng, G.; Montero, A.; Gastaminza, P.; Whitten-Bauer, C.; Wieland, S. F.; Isogawa, M.; Fredericksen, B.; Selvarajah, S.; Gallay, P. A.; Ghadiri, M. R.; Chisari, F. V. A. Virocidal Amphipathic α-Helical Peptide that Inhibits Hepatitis C Virus Infection In Vitro. *Proc. Natl. Acad. Sci. U.S.A.* **2008**, *105*, 3088–3093.

(2) Noueiry, A. O.; Olivo, P. D.; Slomczynska, U.; Zhou, Y.; Buscher, B.; Geiss, B.; Engle, M.; Roth, R. M.; Chung, K. M.; Samuel, M.; Diamond, M. S. Identification of Novel Small-Molecule Inhibitors of West Nile Virus Infection. *J. Virol.* **2007**, *81*, 11992–12004.

(3) Chu, J. J. H.; Yang, P. L. c-Src Protein Kinase Inhibitors Block Assembly and Maturation of Dengue Virus. *Proc. Natl. Acad. Sci. U.S.A.* **2007**, *104*, 3520–3525.

(4) Pierra, C.; Amador, A.; Benzaria, S.; Cretton-Scott, E.; D'Amours, M.; Mao, J.; Mathieu, S.; Moussa, A.; Bridges, E. G.; Standring, D. N.; Sommadossi, J. P.; Storer, R.; Gosselin, G. Synthesis and Pharmacokinetics of Valopicitabine (NM283), an Efficient Prodrug of the Potent Anti-HCV Agent 2′-C-Methylcytidine. *J. Med. Chem.* **2006**, *49*, 6614–6620.

(5) Whitby, K.; Pierson, T. C.; Geiss, B.; Lane, K.; Engle, M.; Zhou, Y.; Doms, R. W.; Diamond, M. S. Castanospermine, a Potent Inhibitor of Dengue Virus Infection In Vitro and In Vivo. *J. Virol.* **2005**, *79*, 8698–8706.

(6) Whitby, K.; Taylor, D.; Patel, D.; Ahmed, P.; Tyms, A. S. Action of Celgosivir (6 *O*-Butanoyl Castanospermine) Against the Pestivirus BVDV: Implications for the Treatment of Hepatitis C. *Antiviral Chem. Chemother.* **2004**, *15*, 141–151.

(7) Bai, F. W.; Wang, T.; Pal, U.; Bao, F.; Gould, L. H.; Fikrig, E. Use of RNA Interference to Prevent Lethal Murine West Nile Virus Infection. *J. Infect. Dis.* **2005**, *191*, 1148–1154.

(8) Leyssen, P.; Balzarini, J.; De Clercq, E.; Neyts, J. The Predominant Mechanism by which Ribavirin Exerts Its Antiviral Activity In Vitro Against Faviviruses and Paramyxoviruses Is Mediated by Inhibition of IMP Dehydrogenase. *J. Virol.* **2005**, *79*, 1943–1947.

(9) Benarroch, D.; Egloff, M. P.; Mulard, L.; Guerreiro, C.; Romette, J. L.; Canard, B. A Structural Basis for the Inhibition of the NS5 Dengue Virus mRNA 2′-*O*-Methyltransferase Domain by Ribavirin 5′-Triphosphate. *J. Biol. Chem.* **2004**, *279*, 35638–35643.

(10) Angusti, A.; Manfredini, S.; Durini, E.; Ciliberti, N.; Vertuani, S.; Solaroli, N.; Pricl, S.; Ferrone, M.; Fermeglia, M.; Loddo, R.; Secci, B.; Visioli, A.; Sanna, T.; Collu, G.; Pezzullo, M.; La.Colla, P. Design, Synthesis, and Anti Flaviviridae Activity of *N*(6)-5′,3′-*O*- and 5′,2′-*O*-Substituted Adenine Nucleoside Analogs. *Chem. Pharm. Bull.* **2008**, *56*, 423–432.

(11) Bai, F. W.; Town, T.; Pradhan, D.; Cox, J.; Ashish; Ledizet, M.; Anderson, J. F.; Flavell, R. A.; Krueger, J. K.; Koski, R. A.; Fikrig, E. Antiviral Peptides Targeting the West Nile Virus Envelope Protein. *J. Virol.* **2007**, *81*, 2047–2055.

(12) Heinz, F. X.; Allison, S. L. Structures and Mechanism in Flavivirus Fusion. *Adv. Virus Res.* **2000**, *55*, 231–269.

(13) Rey, F. A.; Heinz, F. X.; Mandl, C.; Kunz, C.; Harrison, S. C. The Envelope Glycoportein from Tick-borne Encephalitis Virus at 2 Å Resolution. *Nature* **1995**, *375*, 291–298.

(14) Modis, Y.; Ogata, S.; Clements, D.; Harrison, S. C. A. Ligand-Binding Pocket in the Dengue Virus Envelope Glycoprotein. *Proc. Natl. Acad. Sci. U.S.A.* **2003**, *100*, 6986–6991.

(15) Zhang, Y.; Zhang, W.; Ogata, S.; Clements, D.; Strauss, J. H.; Baker, T. S.; Kuhn, R. J.; Rossmann, M. G. Conformational Changes of the Flavivirus E Glycoprotein. *Structure* **2004**, *12*, 1607–1618.

(16) Bressanelli, S.; Stiasny, K.; Allison, S. L.; Stura, E. A.; Duquerroy, S.; Lescar, J.; Heinz, F. X.; Rey, F. A. Structure of a Flavivirus Envelope Glycoprotein in Its Low-pH-Induced Membrane Fusion Conformation. *EMBO J.* **2004**, *23*, 728–738.

(17) Colla, L.; Herdewijn, P.; Declercq, E.; Balzarini, J.; Vanderhaeghe, H. Synthesis and Biological-Activity of 3′-Azido Substituted and 3′-Amino Substituted Nucleoside Analogs. *Eur. J. Med. Chem.* **1985**, *20*, 295–301.

(18) Cecilia, D.; Gould, E. A. Nucleotide Changes Responsible for Loss of Neuroinvasiveness in Japanese Encephalitis-Virus Neutralization-Resistant Mutants. *Virology* **1991**, *181*, 70–77.

(19) Trofimov, B. A.; Schmidt, E. Y.; Vasil'tsov, A. M.; Mikhaleva, A.; Zaitsev, A. B.; Morozova, L. V.; Gorshkov, A. G.; Henkelman, J.; Arndt, J.-D. Synthesis and Properties of *O*-Vinylamidoximes. *Synthesis* **2001**, 2427–2430.

(20) Lee, E.; Weir, R. C.; Dalgarno, L. Changes in the Dengue Virus Major Envelope Protein on Passaging and their Localization on the Three-dimensional Structure of the Protein. *Virology* **1997**, *232*, 281–290.

(21) Beasley, D. W. C.; Aaskov, J. G. Epitopes on the Dengue 1 Virus Envelope Protein Recognized by Neutralizing IgM Monoclonal Antibodies. *Virology* **2001**, *279*, 447–458.

(22) Hurrelbrink, R. J.; McMinn, P. C. Attenuation of Murray Valley Encephalitis Virus by Site-directed Mutagenesis of the Hinge and Putative Receptor-binding Regions of the Envelope Protein. *J. Virol.* **2001**, *75*, 7692–7702.
(23) Monath, T. P.; Arroyo, J.; Levenbook, I.; Zhang, Z. X.; Catalan, J.; Draper, K.; Guirakhoo, F. Single Mutation in the Flavivirus Envelope Protein Hinge Region Increases Neurovirulence for Mice and Monkeys but Decreases Viscerotropism for Monkeys: Relevance to Development and Safety Testing of Live, Attenuated Vaccines. *J. Virol.* **2002**, *76*, 1932–1943.
(24) Okonya, J. F.; Hoffman, R. V.; Johnson, M. C. Synthesis of 2-Oxazolone-4-carboxylates from 3-Nosyloxy- and 3-Bromo-2-ketoesters. *J. Org. Chem.* **2002**, *67*, 1102–1108.
(25) Conover, L. H.; Tarbell, D. S. Thiazole Analogs of Pyridoxine. *J. Am. Chem. Soc.* **1950**, *72*, 5221–5225.
(26) Korytnyk, W.; Angelino, N.; Dave, C.; Caballes, L. Guanylhydrazones with Potential Anti-Leukemic Activity 0.2. Synthesis and Structure−Activity Relationships of Analogs of 4,4′-Diacetyl-*N*,*N*′-Diphenylurea Bis(Guanylhydrazone). *J. Med. Chem.* **1978**, *21*, 507–513.
(27) Cristau, H. J.; Cellier, P. P.; Spindler, J. F.; Taillefer, M. Mild Conditions for Copper-Catalysed N-Arylation of Pyrazoles. *Eur. J. Org. Chem.* **2004**, *69*, 5–709.
(28) Brown, K.; Newberry, R. A. A Novel Synthesis of 4-Hydroxymethyl-2-Phenylthiazole Involving an Epoxy-2-Thiazoline Intermediate. *Tetrahedron Lett.* **1969**, 2797–2708.
(29) Einsiedel, J.; Thomas, C.; Hubner, H.; Gmeiner, P. Phenyloxazoles and phenylthiazoles as benzamide bioisosteres: Synthesis and dopamine receptor binding profiles. *Bioorg. Med. Chem. Lett.* **2000**, *10*, 2041–2044.
(30) De Kimpe, N.; De Cock, W.; Schamp, N. A. A Convenient Synthesis of 1-Chloro-2-alkanones. *Synthesis* **1987**, *2*, 188–190.
(31) Brown, D. J.; Buttler, B. B.; Cowden, W. B.; Grigg, G. W.; Kavulak, D.; Podger, D. M. Unfused Heterobicycles as Amplifiers of Phleomycin. 3. Thiazolylpyridines and Bipyrimidines with Strongly Basic Side Chains. *Aust. J. Chem.* **1981**, *34*, 2423–2429.
(32) Jones, C. T.; Patkar, C. G.; Kuhn, R. J. Construction and Applications of Yellow Fever Virus Replicons. *Virology* **2005**, *331*, 247–259.

JM800412D